

Adaptive transport of folic acid across renal epithelia in folate-deficient rats

Nissar Ahmad Wani · Jyotdeep Kaur

Received: 12 January 2012 / Accepted: 16 July 2012 / Published online: 4 August 2012
© The Physiological Society of Japan and Springer 2012

Abstract Folate (vitamin B₉) is an essential vitamin for a wide spectrum of biochemical reactions; however, unlike bacteria and plants, mammals are devoid of folate biosynthesis and thus must obtain this cofactor from exogenous sources. The activities of folate transporters on the kidneys play an important role in conserving folate excretion and reabsorption across the apical membrane of the renal proximal tubules. The different transport system activities may become identifiable in response to external stimuli, such as folate availability and exposure to chemotherapeutic agents. We have explored the effect of folate deficiency on the activity and expression of folate transporters in rat kidneys. Wistar rats were fed a folate-containing diet (2 mg folic acid kg⁻¹ diet) or a folic acid-free diet over a 3-month period, and mechanisms of folate transport were studied in renal brush border membrane vesicles and basolateral membrane vesicles. The renal folate uptake process is saturable and pH dependent, and it involves the folate receptor and reduced folate carrier (RFC) systems and possibly the proton coupled folate transporter (PCFT) system. We found that folate deficiency increased the renal brush border membrane and basolateral folate uptake by increasing the number of transporter molecules. The observed up-regulation of mRNA expression was also associated with a significant increase in RFC and PCFT expression at the protein level.

Keywords Renal folate uptake · PCFT · RFC · Folate transporters · Folate deficiency · Rats

Introduction

Folic acid is essential for growth, development and normal cellular function, and its uptake is mediated by regulated transport systems [1–3]. Deficiency of this micronutrient can lead to neural tube defects, Alzheimer disease, cardiovascular diseases and cancer [2, 4–8]. Due to the exogenous requirement of folate in mammals, there exists a well-developed epithelial folate transport system for regulation of normal folate homeostasis, including intestinal uptake, renal tubular reabsorption and tissue distribution [3, 9–17]. The renal uptake of folate involves glomerular filtration followed by tubular reabsorption of the filtered folate, which is essential for the conservation and normal homeostasis of this important vitamin [18]. Failure to reabsorb filtered folate would result in urinary losses of approximately 1 mg/day and a subsequent rapid depletion of body stores. Reports have suggested the involvement of a high-affinity folate binding protein (FBP) or folate receptor and a low-affinity transporter, the reduced folate carrier (RFC), as candidate proteins involved in renal folate conservation [11, 19, 20]. However, the role of the high-affinity transporter, i.e. the proton coupled folate transporter, in renal folate conservation remains largely unresolved. In contrast to our understanding of folate uptake under normal conditions, the characteristics of folate uptake under conditions of low dietary intake holds great scope as deficiency of this vitamin is associated with various pathogenesis. The results of previous studies carried out along this line suggest that alterations occur in the WNT/APC pathway under conditions of folate deficiency [21], and a decreased affinity of the folate receptor (FR) or FBP has been observed in tumour tissues of folate-deficient mice [22]. Moreover, folate deficiency in mice was found to result in up-regulated mRNA levels of RFC and proton coupled folate transporter

N. A. Wani · J. Kaur (✉)
Department of Biochemistry, Postgraduate Institute of Medical
Education and Research, Chandigarh 160 012, India
e-mail: jyotdeep2001@yahoo.co.in

(PCFT) in the intestine [23–25]. However, little is known on the mechanisms of renal folate uptake in in vivo models of folate deficiency. We have examined the effect of folate deficiency on the physiology of folate transport in kidneys. The renal folate uptake process is saturable and pH dependent, and it involves the FR and RFC systems and possibly the PCFT system [10, 11]. We found that folate deficiency increased the renal brush border membrane and basolateral folate uptake by increasing the number of transporter molecules without changing their affinity. In addition, the expression of mRNA coding for folate transporters, i.e. *PCFT* and *RFC*, were up-regulated during folate deficiency. The increased mRNA expression during folate deficiency was well substantiated by the results of our PCFT and RFC protein analysis in renal tissue.

Materials and methods

Chemicals

Radiolabelled [3', 5', 7, 9-³H]folic acid and potassium salt with a specific activity of 24.0 Ci/mmol were purchased from Amersham Pharmacia Biotech (Hong Kong). The ColorBurstTM electrophoresis marker (MW 8,000–220,000) was purchased from Sigma Chemical Co (St. Louis, MO), the Total RNA Extraction kit was purchased from Taurus Scientific (Cincinnati, OH), the Moloney Murine Leukemia Virus reverse transcriptase (RevertAidTM M-MuLV RT) kit was purchased from MBI Fermentas, Thermo Fisher Scientific, Waltham, MA) and the RNeasy (RNA stabilization solution) was obtained from Ambion (Austin, TX). Primary antibodies rabbit anti-rat RFC (RFC) and anti-rat PCFT (PCFT) polyclonal antibodies were raised in rabbits in our laboratory [17, 26]. Horseradish peroxidase (HRP)-labelled goat anti-rabbit immunoglobulin G (IgG) secondary antibodies was purchased from G Biosciences (St Louis, MO). The metal-enhanced DAB substrate kit was purchased from Thermo Fisher Scientific.

Animals

Weaning male albino rats (Wistar strain) weighing 40–50 g were obtained from the central animal house of our institute and housed in polypropylene cages in the departmental animal house under hygienic conditions at a controlled temperature (23 ± 1 °C) and humidity (44–55 %). The rats were randomized into two groups of eight animals each. Folate deficiency was obtained in one group of rats by feeding them a folate-deficient diet and 10 g succinylsulfathiazole kg⁻¹ diet for 3 months. Inclusion of succinylsulfathiazole facilitates the induction of severe folate deficiency because this antibiotic eradicates intestinal microflora that

are capable of the de novo synthesis of folate, some of which is incorporated into tissue folate of the host. Animals in the control group were pair fed and received a control diet supplemented with folic acid (2 mg kg⁻¹ diet) and were not given succinylsulfathiazole, as described earlier [27]. The composition of the diet is as described by American Institute of Nutrition (AIN). After 3 months of dietary treatment, the animals were sacrificed under pentothal anesthesia.

The protocol of the study was approved by the Institute Animal Ethics Committee and by the Institutional Biosafety Committee of the Postgraduate Institute of Medical Education and Research, Chandigarh, India.

Preparation of renal brush border membrane vesicles

Rat renal cortical brush border membrane vesicles (BBMV) were prepared by differential centrifugation as described earlier [10, 11], and their purity was checked by alkaline phosphatase assay.

Preparation of renal basolateral membrane vesicles

Basolateral membrane vesicles (BLMV) from kidney was prepared by the self-generating Percoll gradient method [28], as previously described [15, 16]. The intestinal scrapings and minced kidneys were homogenized in ice-cold buffer containing 250 mM mannitol and 12 mM HEPES–Tris, pH 7.4 using a Waring blender for 3 min and then centrifuged at 2,500 g for 20 min. The supernatant was then centrifuged at 22,000 g for 25 min and the resulting fluffy layer of the pellet resuspended in same buffer followed by homogenization in a glass Teflon homogenizer. The resulting homogenate was mixed with percoll at a concentration of 15.4 % and centrifuged at 48,000 g for 2 h. A distinct band of BLMV lipid was seen at the upper one-third of the percoll gradient. This band was aspirated by a syringe and suspended in buffer (100 mM mannitol, 100 mM KCl, 12 mM HEPES–Tris, pH 7.4), and the suspension was centrifuged at 48,000 g for 20 min. The pellet obtained was resuspended in loading buffer containing 280 mM mannitol and 20 mM HEPES–Tris, pH 7.4 and centrifuged at 48,000 g for 20 min twice in order to wash out the residual percoll from the membrane preparation. The final pellet representing purified BLMV was suspended in loading buffer (280 mM mannitol, 20 mM HEPES–Tris, pH 7.4) at 5 mg/mL protein concentration. The purity of the membrane preparations was checked by measuring the specific activities of Na⁺, K⁺-ATPase in BLMV and in the original homogenate.

Orientation of the BBMV and BLMV

In any study of folate transport across the kidney, it is important that the BBMV and BLMV be oriented in the

right direction, i.e. BBMVs should be oriented right side-out and the BLMVs oriented inside-out. To investigate this orientation, we measured the activity of Na⁺, K⁺-ATPase in the BLMV and alkaline phosphatase in the BBMV following preincubation with 1 % bovine serum albumin, 20 mM HEPES–Tris (pH 7.0) and 0–1 mg mL⁻¹ sodium dodecyl sulphate (SDS), as described by Milovic et al. [29]. Maximal Na⁺, K⁺-ATPase activity in BLMV is generally limited by the vesicular nature of the preparation, limiting access of ATP and ions to one face or the other of the transmembrane protein. Detergent is therefore used to make the vesicles permeable to these substrates; we buffered the detergent with BSA to avoid denaturation of the enzymes by SDS. Enzyme activities were then determined over a range of detergent concentrations.

Transport of [3', 5', 7, 9-³H] folic acid

Uptake studies were performed at 37 °C in an incubation buffer containing 100 mM NaCl, 80 mM mannitol, 10 mM HEPES, 10 mM 2-morpholinoethanesulfonic acid, pH 5.0 and 0.5 μM of [3', 5', 7, 9-³H]-folic acid, unless otherwise mentioned. The initial rate of the reaction was measured by stopping the transport reaction at 30 s. For the different specific assays, a 10-μl sample of isolated pancreatic plasma membrane vesicles (50 μg protein) from the control and the ethanol-fed rats was added to the incubation buffer which contained [3', 5', 7, 9-³H]folic acid of a known concentration. The reaction was stopped by adding ice-cold stop solution containing 280 mM mannitol, 20 mM HEPES–Tris, pH 7.4, followed by rapid vacuum filtration. Non-specific binding to the filters was determined by residual filter counts after filtration of the incubation buffer and labelled substrate without vesicles, as described earlier [3, 11]. The radioactivity retained by the filters was determined by liquid scintillation counting (model LS 6500; Beckman Coulter, Fullerton, CA).

Reverse transcriptase-PCR analysis

Total RNA was isolated from the kidney by using the Total RNA Extraction kit (Taurus Scientific), and cDNA synthesis was carried out from the purified and intact total RNA according to manufacturer's instructions. Expression of *RFC*, *PCFT*, *FBP* and glyceraldehyde 3-phosphate dehydrogenase (*GAPDH*) was evaluated using sequence-specific primers corresponding to the sequence in the open reading frame. The PCR mixture (20 μL) was prepared in 1 × PCR buffer containing 0.6 U of *Taq* polymerase, 2 μM of each primer for *GAPDH*, *PCFT*, *RFC* and *FBP*, along with 200 μM of each dNTP. In the optimized PCR analysis, the initial denaturation step was carried out for 2 min at 95 °C; the denaturation, annealing and elongation steps were

carried out respectively for 1 min at 94 °C, 45 s at 64 °C (*PCFT*) or 56 °C (*GAPDH*) and 1 min at 72 °C for 35 cycles. In the case of *RFC* and *FBP* denaturation, the annealing and elongation steps were carried out respectively for 30 s at 94 °C, 30 s at 52.1 °C (*RFC*) or 58 °C (*FBP*), 30 s at 72 °C for 35 cycles. The final extension step was carried out for 10 min at 72 °C. The primers were designed using Primer3 Input ver. 0.4.0 (NCBI–NIH, Bethesda, MD). The sequences of the primers used were as follows: 5'-CATGCTAAGCGAACTGGTGA-3' (sense) and 5'-TTTCCACAGGACATGGACA-3' (antisense) for *RFC*; 5'-AAGCCAGTTATGGGCAACAC-3' (sense) and 5'-GGA TAGGCTGTGGTCAAGGA-3' (antisense) for *PCFT*; 5'-CAACAAGCCAGGAAGACA-3' (sense) and 5'-CAAGT TCGGGGAACACTCAT-3' (antisense) for *FBP*; 5'-CCTTC ATTGACCTCAACTACAT-3' (sense) and 5'-CCAAAGTT GTCATGGATGACC-3' (antisense) for *GAPDH*. The expected PCR products of size 120, 300, 136 and 400 bp were obtained for *RFC*, *PCFT*, *FBP* and *GAPDH*, respectively, when electrophoresed on 1.2 % agarose gel. The densitometric analyses of products were determined by using Image J software (NIH).

Western blot analysis

For the protein expression studies, kidney tissue was lysed in RIPA buffer, and 100 μg protein was resolved on 10 % SDS-polyacrylamide gel electrophoresis (PAGE) and transferred to PVDF membrane for 20 min at 15 V using semidry electroblotter. Western blotting was performed using the procedure described by Towbin [30], with polyclonal primary antibodies as rabbit anti-rat *RFC* (1:800 dilutions) raised against the specific region of rat *RFC* synthetic peptide corresponding to amino acids 494–512 [17, 31]. The polyclonal antibodies against *PCFT* (1:1,000 dilutions) were raised against the specific region of rat *PCFT* synthetic peptide corresponding to amino acids 442–459 [17]. The secondary antibodies used were goat anti-rabbit IgG–HRP-labelled (1:20,000 dilutions). The bands were visualized using either the metal-enhanced DAB substrate kit or enhanced chemiluminescence detection kit according to the manufacturer's instructions. The quantification of blots was carried out by using Image J software.

Statistical analysis

Each uptake assay was performed three times with four independent preparations from each group. Statistical analysis was performed with GraphPad Prism software (GraphPad, La Jolla, CA). The data were computed as the mean ± standard deviation (SD). Group means were compared by using Student's *t* test and analysis of variance

(ANOVA). The acceptable level of significance was 5 % for each analysis.

Results

Orientation of membrane vesicles

Na^+ , K^+ -ATPase and alkaline phosphatase activities were measured in BBMV and BLMV, respectively, following the incubation of the vesicles in the presence of increasing concentrations of SDS. The activity of alkaline phosphatase remained constant up to an SDS concentration of 1 mg mL^{-1} , suggesting that BBMV were right side oriented. However Na^+ , K^+ -ATPase showed increased activity after permeabilization of the vesicles at SDS concentrations over the range $0.5\text{--}0.8 \text{ mg mL}^{-1}$. This result indicates accessibility of the ions to the other side of the membrane, which is required for maximal Na^+ , K^+ -ATPase activity, and therefore suggests that BLMV were oriented inside-out. They consequently resembled an adequate system for the transport studies.

Reabsorption of folate in kidney under folate-deficient conditions

Folate uptake was measured for 30 s at both the BBM and BLM surfaces. The measurement time selected as a time point was just prior to the uptake maxima observed in both groups (data not shown) and revealed a significantly higher folate uptake in folate-deficient rats than in the controls (Fig. 1). In order to determine the driving force for folate transport across the renal BBM and BLM, the pH of the incubation buffer was varied from 4.5 to 8, keeping the intravesicular pH constant at 7.4. As shown in Fig. 2, with increasing hydrogen ion concentration (decreasing pH) across the renal BBM, an increase in folate uptake was observed in both rat groups. This increase was most evident when the uptake changed from pH 7 to a mildly acidic pH 5. Moreover, at the different pH points studied, the folate uptake was 40–54 % higher ($p < 0.001$) in the folate-deficient group than in the control group. In the case of renal BLM, a pH of 6 was found to be the optimum pH for folate uptake across the renal BLM, with a significantly higher uptake in folate-deficient rats (24–60 %; $p < 0.01$, 0.001) (Fig. 3). Since the saturation kinetics is a notable characteristic feature of carrier-mediated transport, we also performed kinetic studies in the presence of increasing concentrations of the substrate (from 0.125 to $2.0 \text{ }\mu\text{M}$). The initial velocity determined at 30 s and at pH 5.0 for BBM and pH 6 for BLM showed that in both groups the saturation phenomenon with a plateau at $1.0 \text{ }\mu\text{M}$ of substrate concentration was indicative of Michaelis–Menten kinetics

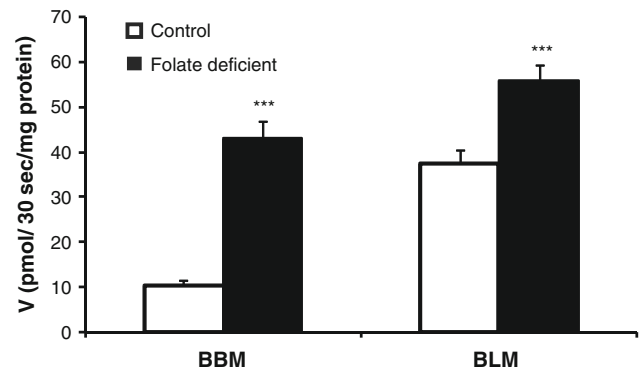


Fig. 1 Folate uptake in the renal brush border membrane vesicles (BBMV) and basolateral membrane vesicles (BLMV). Uptake of [^3H]folic acid ($0.5 \text{ }\mu\text{M}$) was measured in a buffer of pH 5.5 across the BBMV and in a buffer of pH 6.0 across the BLMV (100 mM NaCl, 80 mM mannitol, 10 mM HEPES, 10 mM 2-morpholinoethanesulfonic acid, pH 5.5, 6.0) for 30 s. Data represent the mean \pm standard deviation (SD) of four determinations. *** $p < 0.01$ vs. control

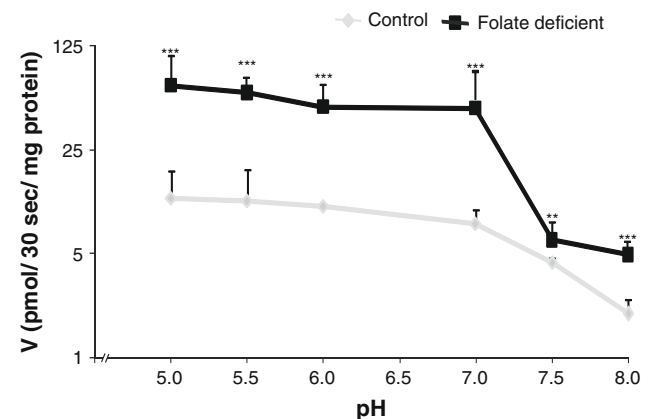


Fig. 2 Uptake of [^3H]folic acid in the BBM as a function of pH optimum. Uptake was measured by varying the pH of the incubation buffer (100 mM NaCl, 80 mM mannitol, 10 mM HEPES, 10 mM 2-morpholinoethanesulfonic acid, pH from 5.0 to 8.0), keeping the intravesicular at pH 7.4, at $0.5 \text{ }\mu\text{M}$ substrate concentration for 30 s. Each data point is the mean \pm SD of four separate uptake determinations. ** $p < 0.01$, *** $p < 0.001$ vs. control. V velocity

(Fig. 4). At the physiological range of folic acid ($0\text{--}1.0 \text{ }\mu\text{M}$), the uptake was 45–81 % higher at the BBM ($p < 0.05$, $p < 0.01$, $p < 0.001$) and 10–45 % higher at the BLM ($p < 0.05$, $p < 0.01$, $p < 0.001$) in the folate-deficient group. In addition, the values of the kinetic constants K_m (Michaelis constant) and V_{max} (maximum velocity of reaction) were determined by nonlinear least square analysis (NLSQ). The K_m values for the control group and group fed the folate-deficient diet were 0.77 ± 0.083 and $0.81 \pm 0.22 \text{ }\mu\text{M}$, respectively, at the BBM and 1.23 ± 0.376 and $1.55 \pm 0.345 \text{ }\mu\text{M}$ at the BLM, respectively. The value of V_{max} for control and folate-deficient rats was 57.23 ± 2.18 and $138.2 \pm 13.73 \text{ pmol/30 s/mg protein}$, respectively, at

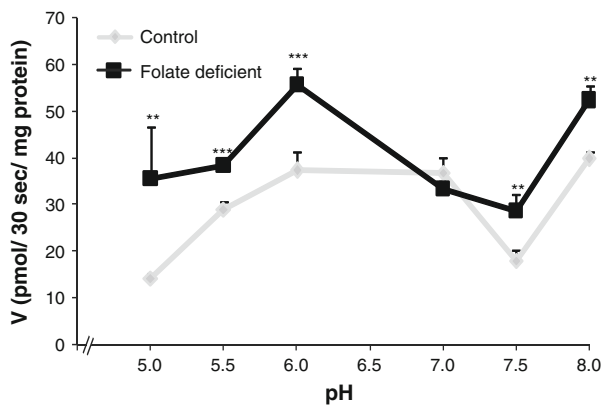


Fig. 3 Uptake of [³H]folic acid in the BLM as a function of pH optimum. Uptake was measured by varying the pH of incubation buffer (100 mM NaCl, 80 mM mannitol, 10 mM HEPES, 10 mM 2-morpholinoethanesulfonic acid, pH from 5.0 to 8.0), keeping the intravesicular at pH 7.4, at 0.5 μM substrate concentration for 30 s. Each data point is mean ± SD of 4 separate uptake determinations. ***p* < 0.01, ****p* < 0.001 vs. control

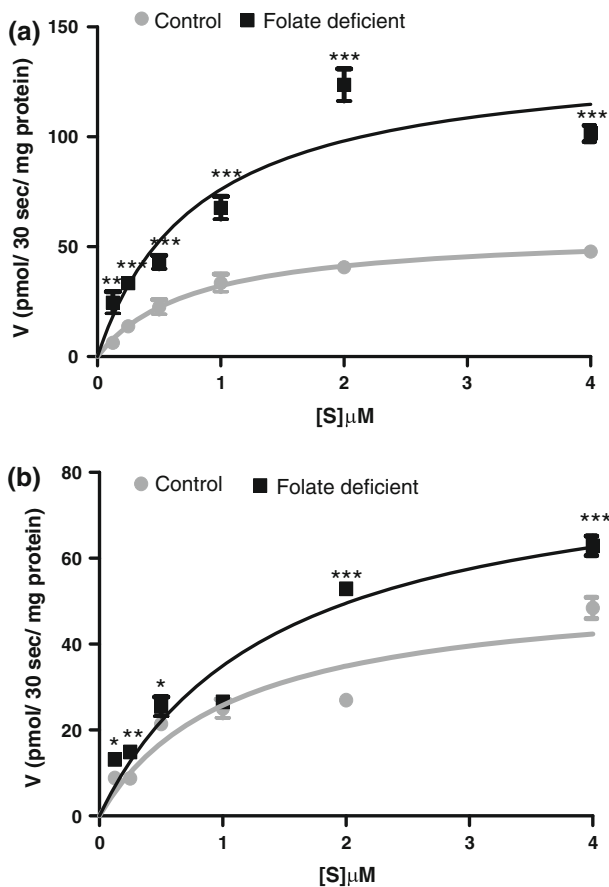


Fig. 4 Uptake of [³H]folic acid in the renal BBM (a) and BLM (b), as a function of substrate (S) concentration. Uptake was measured by varying [³H]folic acid concentration from 0.125 to 4.0 μM in the incubation medium (100 mM NaCl, 80 mM mannitol, 10 mM HEPES, 10 mM 2-morpholinoethanesulfonic acid, pH 5.5 or 6.0) after incubating renal BBMV for 30 s. Each data point is the mean ± SD of 4 separate uptake determinations. **p* < 0.05, ***p* < 0.01, ****p* < 0.001 vs. control

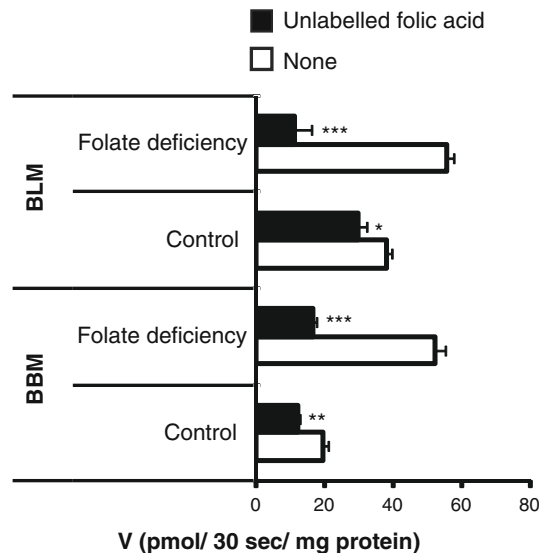


Fig. 5 Uptake of [³H]folic acid in the renal BBM and BLM as a function of the structural analog (unlabelled folic acid). Uptake of [³H]folic acid (0.5 μM) was measured with and without the analog (5 μM folic acid). **p* < 0.05, ***p* < 0.01, ****p* < 0.001 vs. no folic acid

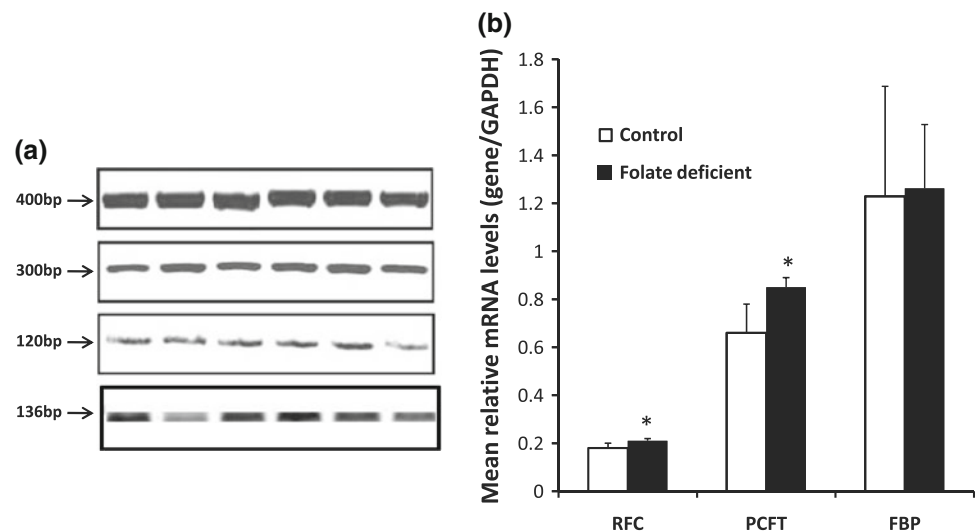
the BBM and 56.14 ± 7.0 and 87.53 ± 8.7 pmol/30 s/mg protein at the BLM, respectively (*p* < 0.001).

In order to determine the specificity of the transport system in renal membrane surfaces (Fig. 5), we measured folate uptake in the presence of the structural analog of unlabelled folic acid. At the renal BBM, the structural analog folic acid decreased the transport by 38 (*p* < 0.01) and 68 % (*p* < 0.001) in the control and folate-deficient rats, respectively; at the renal BLM, the structural analog folic acid decreased the transport by 19 (*p* < 0.05) and 81 % (*p* < 0.001) in the control and folate-deficient rats, respectively.

Expression of mRNA corresponding to *rRFC*, *rPCFT* and *rFBP*

The findings that the folic acid uptake process was markedly increased in renal membrane surfaces with an appreciable increase in *V*_{max} in the folate-deficient group as compared to control led us to determine the mRNA expression of the folate transporters. To this end, we performed reverse transcriptase (RT)-PCR analysis using gene-specific primers for *rRFC*, *rPCFT*, *rFBP* and *rGAPDH* (as internal control). We deduced that there was a significant increase in the expression of mRNA coding for *rRFC* and *rPCFT* in the folate-deficient group (Fig. 6), with 21 (*p* < 0.05) and 13 % (*p* < 0.05) increased expression for PCFT and RFC, respectively (Fig. 6b). However there was no significant change in the mRNA expression of FBP in folate-deficient rats as compared to control rats.

Fig. 6 Reverse transcriptase-PCR analysis of the reduced folate carrier (*RFC*; 120 bp), proton coupled folate transporter (*PCFT*; 300 bp) and folate binding protein (*FBP*; 136 bp), with glyceraldehyde 3-phosphate dehydrogenase (*GAPDH*; 400 bp) as an internal control in kidney. **a** Resolution on 1.2 % agarose gel electrophoresis, **b** densitometric analysis representing relative change in *PCFT*, *RFC* and *FBP* mRNA expression. Data shown are representative of five separate sets of experiments. Lanes: 1–3 Controls, 4–6 folate-deficient rats. * $p < 0.05$ vs. control



Expression of the PCFT and the RFC protein

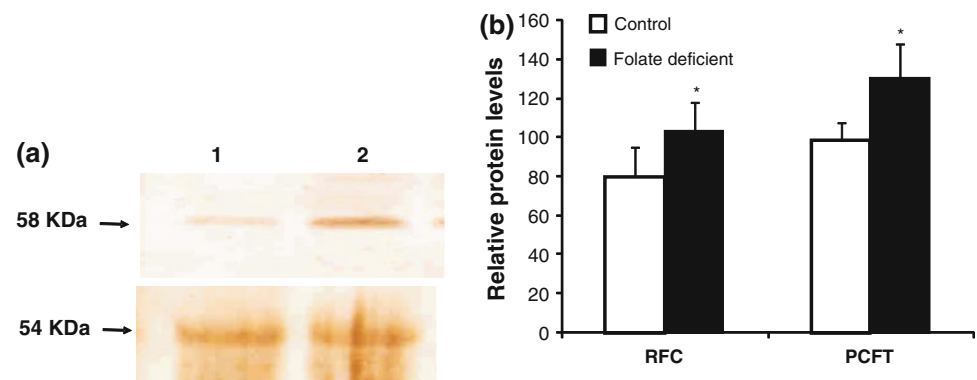
The finding that folate deficiency resulted in a significant increase in mRNA levels of both *PCFT* and *RFC* led us to study whether this increase in mRNA levels was associated with a similar increase in protein levels. We therefore carried out a western blotting assay on renal tissue of both groups of rats (Fig. 7). Parallel to the observed increase in mRNA expression, we found a significant increase in the level of expression of the *PCFT* ($p < 0.05$) and *RFC* ($p < 0.05$) proteins in the renal tissues of the folate-deficient rats (Fig. 7), with *PCFT* expression increasing by 23 % ($p < 0.05$) and *RFC* expression increasing by 26 % ($p < 0.05$) in the folate-deficient rats as compared to the respective controls.

Discussion

Folate-mediated one-carbon metabolism is of fundamental importance for various cellular processes, including DNA

synthesis and methylation [1, 2]. Consequently, the deficiency of this micronutrient might affect gene expression by disrupting DNA methylation patterns or by inducing base substitution and DNA strand breaks [1, 32, 33]. Such changes in expression might explain the inverse relationship observed between folate status and risk of cancers and other diseases, such as neural tube defects, Alzheimer disease and cardiovascular diseases [2, 4–7, 27]. Folate uptake is mediated by regulated transport systems, and the activities of these folate transporters on the renal BBM and BLM play an important role in conserving folate excretion and reabsorption across the proximal tubules [34]. These transport system activities may become distinguishable in response to external stimuli, such as alterations in folate availability and exposure to certain chemotherapeutic agents [2, 35]. Keeping this in view, the aim of our study was to delineate the kinetic behaviour of the folate uptake system across the renal BBM and BLM and the molecular expression of transporters under physiological and folate-deficient conditions. Studying this system holds great potential for increasing our understanding of epithelial

Fig. 7 Western blot analysis of renal tissue using anti-*RFC* (58 kDa) (a) and anti-*PCFT* (54 kDa) (b) antibodies. The graph represents summary data of densitometric analysis. Data are expressed as the mean \pm SD of 4 separate experiments. Lanes: 1 control, 2 folate deficient. * $p < 0.05$ vs. control



folate transport in the kidney under conditions of derangement of folate homeostasis, not only under folate-deficient conditions but also in other renal diseases.

We created a state of folate deficiency by omitting folate from the diet and supplementing the diet with succinylsulfathiazole, which is a nonabsorbed antibiotic that inhibits the *de novo* synthesis of folate by the intestinal microflora. This feeding regimen has been shown in earlier studies to be useful in inducing the folate-deficient state in rats [27, 31]. A prerequisite to carrying out our studies was to isolate renal BBMV and BLMV from rats fed the folate-deficient and ascertain that these were oriented right-side and inside-out, respectively. The permeabilization properties of these vesicles in SDS indicated that they met this criterion and thus represent an adequate and accurate transport system for performing uptake studies. Our results using these vesicles showed a higher uptake in an acidic micro-environment across both the BBM and BLM surfaces, reinforcing earlier observations that an inwardly directed H^+ gradient is necessary for folate uptake across both these membranes and corroborating earlier studies that an acidic microclimate is a necessary factor for operation of the active component of the folate transport system across renal BBM and BLM [10, 11]. The up-regulation of folate uptake in the renal BBM and BLM was associated with an increase in number of transporter molecules (higher V_{max}) without any change in the affinity of the transporter molecules towards its substrate, which is in accordance with previous studies carried out in intestine (in preparation). The K_m values observed at the renal BBM here might represent the affinity of PCFT and FBP for folic acid, while those at BLM might represent the affinity of RFC and PCFT. Moreover, in accordance with our earlier studies [10], the slightly lower K_m values at the renal BBM compared to BLM suggests a more efficient folate uptake system across the BBM as compared to the BLM. For the assessment of the specificity of the folate transport system, the addition of unlabelled folic acid to the incubation medium significantly reduced folate uptake in both groups and at both membrane surfaces, with a greater decrease in rats fed a folate-deficient diet. The possible reason for this decrease could be an increase in the affinity of folate transporters for the unlabelled folic acid in the folate-deficient rats. However, the exact mechanism for process cannot be ascertained with the present data.

The expression profiles of folate transporters PCFT and RFC are of prime importance in any evaluation of the molecular mechanisms involved in the up-regulation of folate uptake, as both are believed to be the transporters responsible for folate uptake across the renal BBM and BLM. In this context, the observed up-regulation in PCFT and RFC mRNA levels was associated with increased expression of both these transporter proteins in the kidney

of rats fed the folate-deficient diet. However, there was no change in the mRNA expression of FBP. The increase in the expression of PCFT and RFC transporters might reflect activation of some transcriptional, translational or post-translational event after the folate deficiency condition was reached in rats. Such findings demand a molecular mechanistic understanding, which could explain the role of expression of the transporter molecules in renal tissue during folate deficiency. Further studies addressing the molecular regulation of RFC, FBP and PCFT synthesis and trafficking during folate deficiency are required to evaluate the site of transcriptional regulation.

Conclusion

In summary, folate deficiency in rats leads to increased renal BBM and BLM folate uptake as a result of the increased mRNA expression of RFC and PCFT, which was in turn associated with increased levels of protein.

Acknowledgments The financial assistance from Indian council of Medical Research, New Delhi, India is highly acknowledged.

Conflict of interest The authors declare that they have no competing interests.

References

1. Hamid A, Wani NA, Kaur J (2009) New perspectives on folate transport in relation to alcoholism-induced folate malabsorption—association with epigenome stability and cancer development. *FEBS J* 276:2175–2191
2. Wani NA, Hamid A, Kaur J (2008) Folate status in various pathophysiological conditions. *IUBMB Life* 60:834–842
3. Wani NA, Nada R, Kaur J (2011) Biochemical and molecular mechanisms of folate transport in rat pancreas; interference with ethanol ingestion. *PLoS One* 6:e28599
4. Cravo ML, Mason JB, Dayal Y, Hutchinson M, Smith D et al (1992) Folate deficiency enhances the development of colonic neoplasia in dimethylhydrazine-treated rats. *Cancer Res* 52:5002–5006
5. Davis CD, Uthus EO (2004) DNA methylation, cancer susceptibility, and nutrient interactions. *Exp Biol Med* (Maywood) 229:988–995
6. Daly LE, Kirke PN, Molloy A, Weir DG, Scott JM (1995) Folate levels and neural tube defects. Implications for prevention. *JAMA* 274:1698–1702
7. Daly S, Mills JL, Molloy AM, Conley M, Lee YJ et al (1997) Minimum effective dose of folic acid for food fortification to prevent neural-tube defects. *Lancet* 350:1666–1669
8. Djukic A (2007) Folate-responsive neurologic diseases. *Pediatr Neurol* 37:387–397
9. Hamid A, Kaur J (2005) Kinetic characteristics of folate binding to rat renal brush border membrane in chronic alcoholism. *Mol Cell Biochem* 280:219–225

10. Hamid A, Kaur J (2006) Chronic alcoholism alters the transport characteristics of folate in rat renal brush border membrane. *Alcohol* 38:59–66
11. Hamid A, Kaur J (2007) Decreased expression of transporters reduces folate uptake across renal absorptive surfaces in experimental alcoholism. *J Membr Biol* 220:69–77
12. Hamid A, Kaur J (2007) Long-term alcohol ingestion alters the folate-binding kinetics in intestinal brush border membrane in experimental alcoholism. *Alcohol* 41:441–446
13. Hamid A, Kaur J (2009) Role of signaling pathways in the regulation of folate transport in ethanol-fed rats. *J Nutr Biochem* 20: 291–297
14. Hamid A, Kiran M, Rana S, Kaur J (2009) Low folate transport across intestinal basolateral surface is associated with down-regulation of reduced folate carrier in in vivo model of folate malabsorption. *IUBMB Life* 61:236–243
15. Hamid A, Wani NA, Rana S, Vaiphei K, Mahmood A et al (2007) Down-regulation of reduced folate carrier may result in folate malabsorption across intestinal brush border membrane during experimental alcoholism. *FEBS J* 274:6317–6328
16. Wani NA, Hamid A, Khanduja KL, Kaur J (2012) Folate malabsorption is associated with down-regulation of folate transporter expression and function at colon basolateral membrane in rats. *Br J Nutr* 107:800–808
17. Wani NA, Kaur J (2011) Reduced levels of folate transporters (PCFT and RFC) in membrane lipid rafts result in colonic folate malabsorption in chronic alcoholism. *J Cell Physiol* 226:579–587
18. Sabharanjak S, Mayor S (2004) Folate receptor endocytosis and trafficking. *Adv Drug Deliv Rev* 56:1099–1109
19. Elwood PC, Deutsch JC, Kolhouse JF (1991) The conversion of the human membrane-associated folate binding protein (folate receptor) to the soluble folate binding protein by a membrane-associated metalloprotease. *J Biol Chem* 266:2346–2353
20. Wang Y, Zhao R, Russell RG, Goldman ID (2001) Localization of the murine reduced folate carrier as assessed by immunohistochemical analysis. *Biochim Biophys Acta* 1513:49–54
21. Crott JW, Liu Z, Keyes MK, Choi SW, Jang H et al (2008) Moderate folate depletion modulates the expression of selected genes involved in cell cycle, intracellular signaling and folate uptake in human colonic epithelial cell lines. *J Nutr Biochem* 19: 328–335
22. Gates SB, Mendelsohn LG, Shackelford KA, Habeck LL, Kursar JD et al (1996) Characterization of folate receptor from normal and neoplastic murine tissue: influence of dietary folate on folate receptor expression. *Clin Cancer Res* 2:1135–1141
23. Subramanian VS, Chatterjee N, Said HM (2003) Folate uptake in the human intestine: promoter activity and effect of folate deficiency. *J Cell Physiol* 196:403–408
24. Qiu A, Min SH, Jansen M, Malhotra U, Tsai E et al (2007) Rodent intestinal folate transporters (SLC46A1): secondary structure, functional properties, and response to dietary folate restriction. *Am J Physiol Cell Physiol* 293:C1669–C1678
25. Liu M, Ge Y, Cabelof DC, Aboukameel A, Heydari AR et al (2005) Structure and regulation of the murine reduced folate carrier gene: identification of four noncoding exons and promoters and regulation by dietary folates. *J Biol Chem* 280: 5588–5597
26. Dev S, Ahmad Wani N, Kaur J (2011) Regulatory mechanisms of intestinal folate uptake in a rat model of folate oversupplementation. *Br J Nutr* 105:827–835
27. Singla A, Kaushik S, Kaur J (2006) Folate deficiency results in alteration in intestinal brush border membrane composition and enzyme activities in weanling rats. *J Nutr Sci Vitaminol (Tokyo)* 52:163–167
28. Scalera V, Storelli C, Storelli-Joss C, Haase W, Murer H (1980) A simple and fast method for the isolation of basolateral plasma membranes from rat small-intestinal epithelial cells. *Biochem J* 186:177–181
29. Milovic V, Stein J, Piiper A, Gerhard R, Zeuzem S et al (1995) Characterization of putrescine transport across the intestinal epithelium: study using isolated brush border and basolateral membrane vesicles of the enterocyte. *Eur J Clin Invest* 25:97–105
30. Towbin H, Staehelin T, Gordon J (1992) Electrophoretic transfer of proteins from polyacrylamide gels to nitrocellulose sheets: procedure and some applications. *Biotechnology* 24:145–149
31. Said HM, Chatterjee N, Haq RU, Subramanian VS, Ortiz A et al (2000) Adaptive regulation of intestinal folate uptake: effect of dietary folate deficiency. *Am J Physiol Cell Physiol* 279:C1889–C1895
32. Moretti P, Sahoo T, Hyland K, Bottiglieri T, Peters S et al (2005) Cerebral folate deficiency with developmental delay, autism, and response to folinic acid. *Neurology* 64:1088–1090
33. Mangold S, Blau N, Opladen T, Steinfeld R, Wessling B et al (2011) Cerebral folate deficiency: a neurometabolic syndrome? *Mol Genet Metab* 104:369–372
34. Sikka PK, McMartin KE (1998) Determination of folate transport pathways in cultured rat proximal tubule cells. *Chem Biol Interact* 114:15–31
35. Wang ES, O'Connor O, She Y, Zelenetz AD, Sirotiak FM et al (2003) Activity of a novel anti-folate (PDX, 10-propargyl 10-deazaaminopterin) against human lymphoma is superior to methotrexate and correlates with tumor RFC-1 gene expression. *Leuk Lymphoma* 44:1027–1035